

# Implementation of a Correlation-based Decentralized Damage Detection Method Using Wireless Sensors

Nestor E. Castaneda<sup>1</sup>, Fei Sun<sup>1</sup>, Shirley Dyke<sup>2</sup>, Chenyang Lu<sup>3</sup>,  
Austin Hope<sup>4</sup> and Tomonori Nagayama<sup>5</sup>

<sup>1,2,3,4</sup>*Washington University in St. Louis, St. Louis, Missouri 63130 USA*

<sup>5</sup>*University of Tokyo, Tokyo JAPAN*

## **ABSTRACT**

Wireless sensor networks (WSN) are gradually gaining the attention of structural engineers as an attractive tool for structural health monitoring (SHM) applications. In this work, an experimental implementation of a correlation-based, decentralized damage detection technique using a wireless sensor network is presented. The Damage Location Assurance Criterion (DLAC) method is validated experimentally using wireless sensor networks. The networks are deployed on both a steel cantilever beam and on a 3D truss model. The experimental implementations are described and corresponding results are presented. Limitations with sensor functionalities during experiment are also addressed and discussed.

## **1. INTRODUCTION**

Reliable structural integrity assessment typically demands the use of a large number of sensors distributed over the entire structure. As more sensors are used on a structure, the quality and accuracy of the damage information increases. Due to the high cost associated with installation, the number of wired sensors that can be used in SHM applications is limited. Thus, wireless sensors appear to be a very suitable option for structural monitoring because they can be deployed in large numbers at relatively low cost. Powered wireless sensors based on micro-electro-mechanical systems (MEMS) and microprocessors can perform damage detection tasks efficiently by taking advantage of their on-board processing and wireless communication capabilities. Microprocessors are used to accomplish on-board digital signal processing, data aggregation and self-operative functions. Wireless communication enables sensors to transmit processed information for additional analysis and decision fusion.

Despite significant technological advances, constraints in WSN functionalities still demand further investigation to ensure real-time implementation. New techniques in wireless network protocols, time synchronization among sensors, and data aggregation must be implemented for WSN to achieve reliable operation and expand their applicability (Nagayama, 2007). Common centralized and decentralized WSN architectures are being replaced with hierarchical approaches where sensors are assigned in groups with hierarchical roles and deployed over the entire structure (Nagayama, 2007). This approach eliminates the need for transmitting large amounts of data, while still using all available spatial information. However, power is a severely limited resource in wireless sensors. Consequently, power management approaches should account for adaptable energy distributions based on the network needs.

---

1. Graduate Research Assistant, 2. Professor, 3. Assistant Professor, 4. Research Assistant,  
5. Assistant Professor

In this study, wireless sensors network is implemented to experimentally validate a correlation-based, decentralized damage detection algorithm. The present study proposes a two-level analysis where a level one analysis uses the on-board microprocessor resources to perform signal processing analysis and frequency domain curve fitting techniques using the raw data. As a result, limited numbers of intermediate parameters are transmitted wirelessly to the base station, where a level two analysis examines correlation factors and detects damage. In this study, the proposed wireless sensor network architecture is described, limitations observed during experiments are reported, the correlation-based technique implementation is illustrated and the final results for two experiments are presented and discussed.

## **2. WIRELESS SENSOR NETWORK IMPLEMENTATION**

The implementation used in this study employs *iMote2* wireless sensor platforms, a gateway mote and a PC as a base station. Every mote runs a program (implemented in the *nesC* programming language) to partially process the acceleration data acquired from on-board accelerometers. Acceleration data is collected by a digital sensor board at a specific sampling frequency. Digital acceleration data, acquired within frames of 2048 points, is then stored in the local memory. On-board digital signal processing is performed on the stored data to obtain a set of intermediate parameters, which are then transmitted to the base station to complete the algorithm. The wireless sensors communicate with the PC through a gateway mote. The gateway mote receives the data packets from the wireless sensors through wireless communication and relay the data to the PC over a USB cable. The PC base station completes the rest of the damage detection algorithm using a java application to calculate and visualize the final results.

Although the purpose of this study is to validate a decentralized method, raw data is also transmitted to the base station for debugging and validation. Therefore, a reliable transport layer is implemented to achieve reliable data transmission from wireless sensors to the base station. This reliable transport layer is tailored for the specific features of the *TinyOS 1.x* operating system and the *iMote2* wireless sensor platform. The transport layer divides sensor data into packets small enough for the radio protocol stack to handle, transmits all the data packets to the base station, and reassembles them upon arrival. Additionally, the Automatic Repeat Request protocol (ARQ) is implemented to detect and retransmit lost packets during communication. After a sender sends a data packet to the base station, it waits for an acknowledgment from the receiver. If an acknowledgment is not received within a half of second, it will retransmit the data packet. This process is repeated until an acknowledgment is received, at which time the sender mote proceeds to the next data packet. In order to detect duplicate data packets, each data packet has a sequence number differentiating it from the other packets. Therefore, the base station accurately reassembles the original block of data after all of the packets are received. Each packet consists of 15-bytes of data, and a sequence number for a final re-assemble process. For this study, sender *iMote2* motes are configured to send a 12,352 byte block data to the base station divided into 12288 bytes for raw data and 64 bytes for the header.

The reliable communication protocol was verified in a first experimental validation using seven wireless sensors, located 16 feet away from the base station. Various obstacles like a metal bookcase were placed between the base station and the wireless sensor deployment to observe the performance. To detect communication failures, a pattern of bytes was written into the block data before sending it to the base station which is configured to verify if the pattern of bytes still exists after transmission is concluded. The pattern of bytes used was a counter that repeatedly goes from 0x00 to 0xFF. Through the test, each of the seven *iMote2* wireless sensor

sent their block data to the base station sequentially. All of the data from the network arrived successfully, which confirmed a reliable communication protocol.

A java interface was also developed as a user-interface to monitor and control the entire network and define the sensing parameters. Fig. 1 shows the user-interface developed for this implementation. The proposed interface enable users to define sampling frequencies for sensor boards, set curve fitting intervals on frequency domain, initialize the application and save results for post-processing. Additionally, raw and corresponding power spectrum data can be also saved for debugging purposes as mentioned previously.



Fig. 1. User-interface

A severe constraint during the experimental implementations was due to the power. Therefore, in these experimental implementations, a reliable energy supply for the entire network is accomplished using USB cables on at each mote. It must be emphasized that wireless communication is still employed in all implementations.

## 2.2 *iMote2* Platform

Successful SHM applications strongly depend on accurate determination of modal information. Several tasks such as sensing, data processing and flexible communication protocols are required to determine the actual condition and subsequent damage prediction on structures. The smart sensor *iMote2* encompasses all of these requirements in one platform. The *iMote2* (IPR2400) is an advanced wireless sensor platform which offers adequate processing and communication resources to continuously monitor civil infrastructure under intensive conditions. Its main board combines a low power PXA271 XScale processor with an 802.15.4 radio (CC2420) and an antenna using 2.4 GHz. It also offers 256 KB of integrated SRAM and 32 MB of external SDRAM. Important *iMote2* main board features can be observed in Table 1.

A photo of the unit is shown in Fig. 2. Power can be provided by a battery board or via the integrated USB interface. The *iMote2*'s compact size of 48 x 36 x 7 mm makes it a modular and stackable platform which possesses analog and digital interface connectors to interact with sensor and battery boards.

Table 1. *iMote2* Main Board Properties

Microprocessor	XscalePXA271
Active Power (mW)	44 @ 13 MHz, 570 @ 416 MHz
Clock speed (MHz)	13 - 416
RAM (bytes)	256 K + 32 M external
Program flash (bytes)	32 M
802.15.4 radio (ChipCon 2420)	

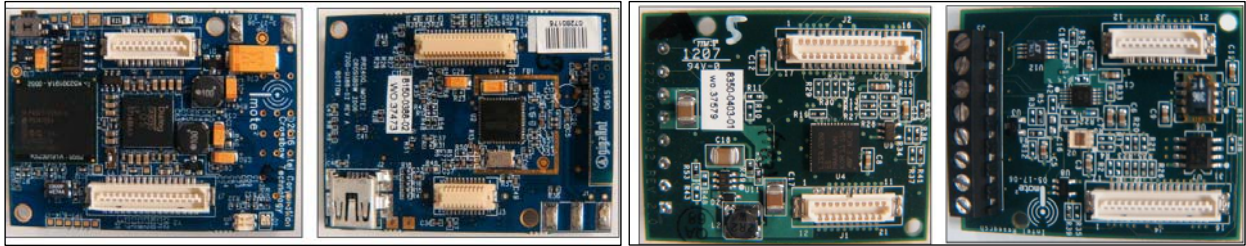


Fig. 2. Top and bottom view of *iMote2* main board and general sensor board

The general sensor board has digital accelerometer, temperature, and humidity and light sensors on board with 4 analog input applications. The accelerometer has a resolution of 12-bit or equivalent 0.97 mg with 3-axis of measurement and  $\pm 2g$  of amplitude. The AD converter has also digital filters with user-defined cutoff frequencies. Sampling frequencies can be calibrated by using a pre-defined decimation factor as observed in Table 2.

Table 2. Accelerometer user specified sampling rates and cutoff frequencies

Decimation Factor	Cutoff Frequency (Hz)	Sampling Rate (Hz)
128	70	280
64	140	560
32	280	1120
8	1120	4480

Specifications for the accelerometer explain that once the decimation factor is defined, the sampling frequency and corresponding cutoff frequency will have a value within  $\pm 10\%$  of the value given. Therefore, a previous general sensor calibration for sampling frequencies of 280Hz and 560Hz was performed by using an oscilloscope.

### 3. CORRELATION-BASED DAMAGE DETECTION TECHNIQUE

SHM techniques can detect, localize and quantify structural damage by analyzing modal content information of the structure. Correlation-based damage detection techniques identify damage by comparing changes on modal parameters obtained by experimental and numerical approaches. Messina proposed the Damage Location Assurance Criterion (DLAC) in 1992 as an adaptation of the Modal Assurance Criterion (MAC) (Contursi, 1998) technique for damage detection. MAC measurements are usually used to validate the accuracy of analytical models produced by experimental tests while DLAC approach identify damage by evaluating the linear correlation between frequency change vectors obtained by experimental measurements and an

analytical model. Therefore, a damage detection pattern is initially required to numerically produce frequency change vectors between the healthy and several damaged conditions. The resultant damage detection pattern, called the sensitivity matrix, describes an array of natural frequencies estimated when a damage hypothesis is simulated on several positions of the analytical model. The final estimation for the linear correlation between frequency change vectors is accomplished by the DLAC equation which is restricted to positive values between 0 and 1. DLAC values close to unity indicate a strong correlation and therefore a potential damage location. The DLAC equation is given as Eq.(1)

$$DLAC_j = \frac{|\{\Delta\omega\}^T \{\delta\omega_j\}|^2}{(\{\Delta\omega\}^T \{\Delta\omega\})(\{\delta\omega_j\}^T \{\delta\omega_j\})} \quad (1)$$

Frequency change vectors for both experimental and numerical models are denoted by  $\Delta\omega$  and  $\delta\omega_j$ , respectively. These vectors are normalized with respect to the healthy natural frequencies using the Eq.(2) to equally weight all vectors and reduce any bias induced by higher modes. Therefore, the DLAC's ability to detect damage is independent of the damage hypothesis because frequency change vectors are normalized and their magnitude is unnecessary for the calculation. Because the DLAC approach is only used to detect individual damage events, other techniques would be implemented to detect multiple damage locations (Koh, 2004). However, damage detection results based on correlation measurements may not be unique in some cases. When a reduced number of modes are considered, combined damage locations could produce the same frequency change vectors as that of one damage location limiting the assessment of a real structural damage location.

$$\Delta\omega = (\omega_{healthy} - \omega_{damage}) / \omega_{healthy} \quad (2)$$

### 3.1 DLAC Implementation

In this study, a two-level approach is developed to implement the DLAC technique for damage detection. A level one analysis partially extracts the modal information of the structure using acceleration records and on-board processing capacity of the wireless sensors. A second level analysis finishes the calculation of the natural frequencies and performs damage detection tasks at the base station. A general flow chart of the entire implementation is provided in Fig. 3. Acceleration time history records are transformed to frequency domain by applying a Fast Fourier Transform (FFT). Power spectrum density (PSD) functions are then calculated as the squared magnitude of the complex FFT values. Finally, a curve fitting technique is applied to the PSD function to determine resonant frequencies locations. A set of intermediate curve fitting parameters are then transmitted wirelessly to the base station where final roots extraction is finished and DLAC values are reported.

Levi's approach is used to accomplish the curve fitting. This complex-curve fitting technique extracts the modal properties from system transfer functions by implementing a fractional polynomial " $G(i\omega)$ " depicted in Eq.(3).

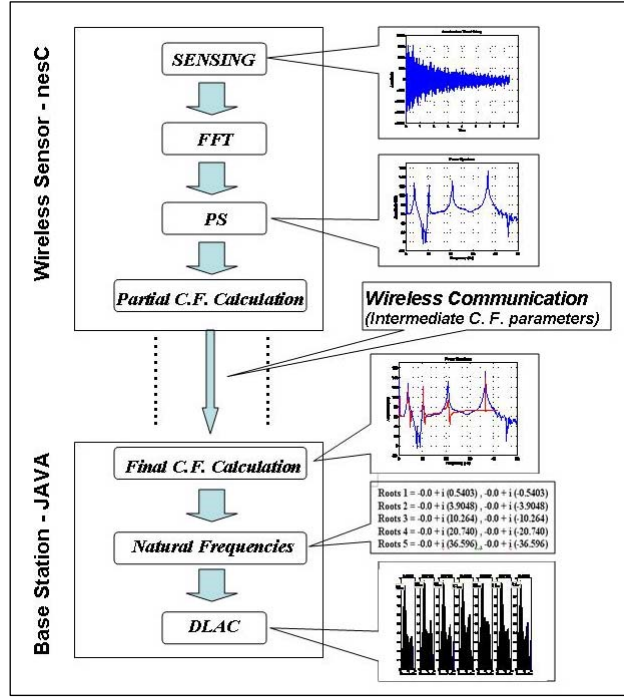


Fig. 3. Flow chart of implementation

The fractional polynomial is defined as the ratio of two complex polynomials in terms of unknown coefficients  $X_i$ ,  $Y_i$  and the frequency variable " $i\omega$ ". The denominator has a polynomial order proportional to the number of resonant frequencies to be captured. If the unknown coefficients of " $G(i\omega)$ " are obtained, natural frequencies are detected by solving the corresponding denominator roots. This technique can also be expanded for PSD curve fitting calculations by considering the complex part of the FFT as a zero value.

$$G(i\omega) = \frac{X_0 + X_1(i\omega) + X_2(i\omega)^2 + X_3(i\omega)^3 + X_4(i\omega)^4 + \dots X_n(i\omega)^n}{Y_0 + Y_1(i\omega) + Y_2(i\omega)^2 + Y_3(i\omega)^3 + Y_4(i\omega)^4 + \dots X_m(i\omega)^m} \quad (3)$$

The fractional polynomial coefficients are obtained by minimizing the weighted sum of the squares errors between the magnitude of the proposed " $G(i\omega)$ " and the experimental transfer function over the frequency domain. Once the error function is minimized, a set of linear transformations are performed to determine the unknown coefficients. Linear transformation coefficients are calculated based on the PSD and corresponding frequency vector. In this study, a second-order fractional polynomial is implemented to capture natural frequencies in five frequency ranges. Linear transformation coefficients associated with the PSD are calculated *in situ* and are wirelessly transmitted back to the base station as intermediate curve fitting parameters. Upon their arrival final roots calculation is completed and DLAC factors calculated.

#### 4. EXPERIMENTAL VALIDATION

Experimental validation of the performance of the DLAC damage detection algorithm has been conducted using a wireless sensor network on two experimental structures of increasing complexity.

#### **4.1 EXPERIMENT 1: Cantilevered Beam**

A steel cantilever beam is selected as the first experimental model to be tested at the Structural Control and Earthquake Engineering Lab at Washington University in St. Louis. The beam model with 108" of length, 3" of width and ¼" of thickness is fixed to the ground to approximate a cantilever support. Seven *iMote2* wireless sensors are attached to the beam to measure acceleration data in a parallel direction to the weaker axis of bending and placed at constant intervals of 15 in measured from the beam support. Sensor boards are calibrated with a sampling frequency of 280 Hz and corresponding cutoff frequency of 70 Hz to independently examine three damage scenarios under impact testing. Every damage scenario is simulated by attaching a small steel bar with an equivalent weight of 1.50 kg placed on the beam at distances of: 26" (D1), 53" (D2), and 74.6" (D3), respectively, as measured from the beam support. The complete experimental set up is depicted in Fig. 4.

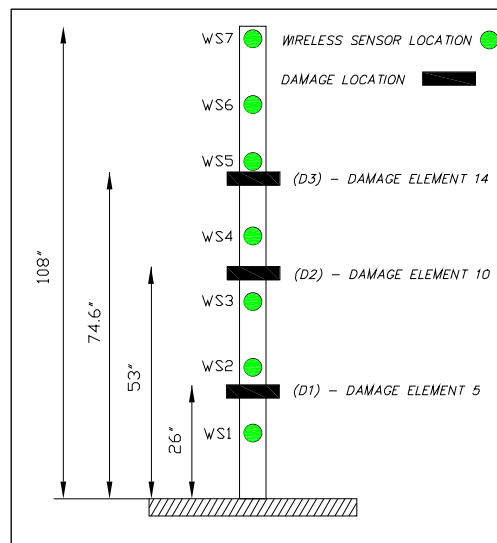


Fig. 4. Diagram of cantilever beam test structure

A numerical model is also developed to yield the healthy and damaged analytical natural frequencies for later correlation comparisons with the DLAC technique. A 2D Bernoulli beam element with transverse and rotational degrees of freedom (DOF) is selected to produce a consistent mass matrix finite element model with 20 elements and 42 global degrees of freedom (see Fig. 5). Boundary conditions are modeled as a cantilever support and translational-rotational DOF are defined for each node.

The numerical model is then used to produce an analytical damage detection pattern for 20 damage scenarios, as required by the DLAC approach. Analytical damage is produced in the model by increasing the density concentration, equivalent to a mass increase of only 67% (1.00 kg) of the actual experimental value (1.50 Kg) at each of the 20 beam elements. The eigenproblem is solved to obtain the healthy natural frequencies and a sensitivity matrix containing information about the first five bending natural frequencies over the 20 beam damage locations. The actual experimental damage, placed at positions already mentioned, is associated with elements 5 (D1), 10 (D2) and 14 (D3) on the FEM. Therefore, final correlation results are expected to be closest to unity for those positions due to the presence of damage. Analytical natural frequency results are depicted in Table 3.

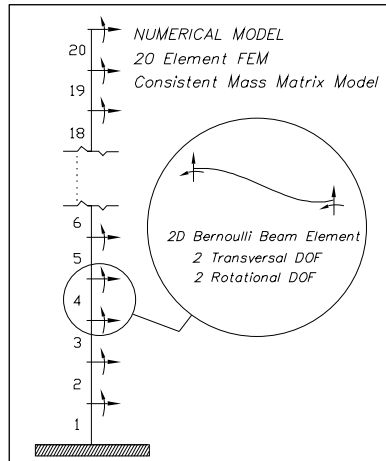


Fig 5. Cantilever beam finite element model

Table. 3. Analytical natural frequencies

Mode	Healthy	D1	D2	D3
1	0.6564	0.6555	0.6443	0.6200
2	4.1133	4.0105	3.7649	4.0026
3	11.5180	10.6192	11.4581	10.7937
4	22.5710	20.8768	21.0991	22.3574
5	37.3160	36.1469	36.8913	36.1677

The first experimental test performed is to experimentally calculate the healthy natural frequencies of the beam. A hammer strike is applied along the weaker bending axis of the beam to approximate an impulse response and ensure a total modal content excitation. The first five healthy natural frequencies, shown in Table 4, are determined by averaging the results from all of the sensors. Differences between the analytical and experimental healthy natural frequencies can be explained due to some numerical assumptions in the analytical model. Boundary conditions, homogeneous distribution for density and constitutive laws, and disregarding numerical modeling for the sensor platforms are the most important causes for those discrepancies. However, damage detection results will demonstrate that the DLAC algorithm is reliable and robust to account for numerical model imperfections even when differences are large (Clayton, 2006); here the errors range from 18% in the fundamental mode to 0.3% in higher modes. In general, damage detection algorithms are required to show reliable robustness to account for numerical model imperfections.

Table 4. Experimental healthy natural frequencies

Mode	1	2	3	4	5
$\omega_n$	0.5381	4.0240	11.4705	22.5506	37.4316

Mass is then attached to the beam to test the DLAC performance under the three different scenarios already described. Because the DLAC is used to detect individual events, each scenario is tested separately. Impact testing is again selected to perform the validation for each



damage case by applying a hammer strike along the weaker bending axis. Results reported using the entire network are depicted in Figs. 6, 7 and 8 where corresponding identified natural frequencies and DLAC measurements are introduced for each damage scenario. DLAC values determined at sensors along the length of the beam are provided. Values close to unity indicate damage location. The entire network report successful damage detection results for all damage scenarios with correlation measurements greater than 90% at the damaged positions. Recall experimental damage positions **D1**, **D2** and **D3** are associated with elements **5**, **10** and **14**, respectively. Despite consistency in the results, some of the sensors report correlation measurements greater than 50% for some of the element positions. As explained previously, results of correlation-based methods may not be unique. Frequency change vectors associated with one damage location could be potentially the same as those obtained with several combinations of damage location when reduced numbers of modes are used. Therefore, the inclusion of more modes is expected to clarify the results by concentrating the correlation measurements around one damage location. Note that these results are obtained with a damage hypothesis of only 67% of the actual damage. Two additional damage hypotheses are implemented to test the DLAC performance off-line using different damage assumptions and acceleration records previously obtained for debugging purposes. New sensitivities matrices and corresponding frequency change vectors were developed with a prescribed analytical damages equivalent to 200% and 33% of the actual damage. Results showed the same tendencies and consistency, and were also successful for all damage scenarios with high correlation measurements.

Mode	WS1	WS2	WS3	WS4	WS5	WS6	WS7
1	0.5506	0.5374	0.5402	0.5316	0.5371	0.5427	0.5392
2	3.9043	3.8902	3.8977	3.8564	3.7678	3.8488	3.9012
3	10.2473	10.2779	10.2714	10.2744	10.0707	10.3217	10.2533
4	20.7641	20.8096	20.7964	20.8470	20.4038	20.7546	20.7751
5	36.6415	36.6396	36.6048	36.6785	35.9797	36.5919	36.6570

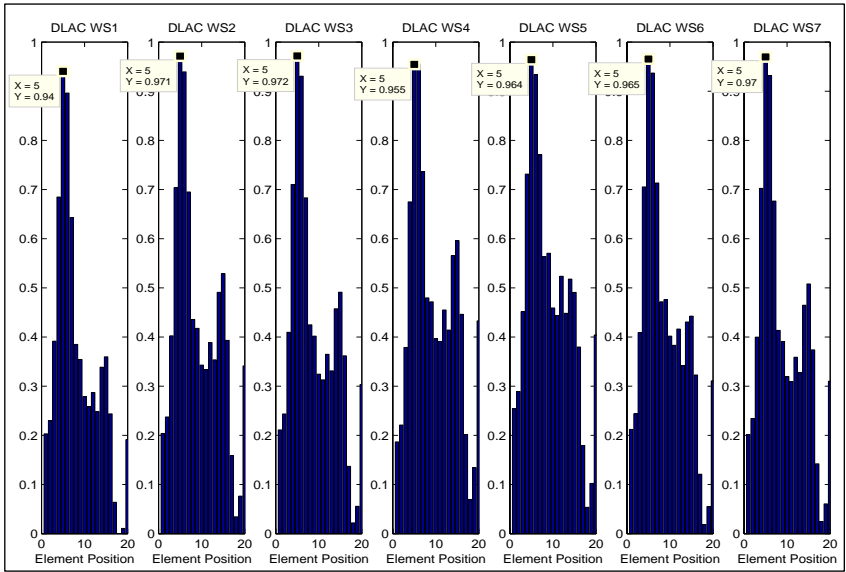


Fig 6. DLAC results for element position # 5

Mode	WS1	WS2	WS3	WS4	WS5	WS6	WS7
1	0.5498	0.5393	0.5386	0.5318	0.5353	0.5420	0.5379
2	3.6042	3.6241	3.6343	3.5979	3.7358	3.5478	3.6284
3	11.4766	11.4127	11.4758	11.4310	11.2721	11.3961	11.4565
4	20.7626	20.7606	20.7952	20.7798	20.4008	20.7528	20.7586
5	37.2342	37.2030	37.2573	37.2568	36.6449	37.1650	37.2391

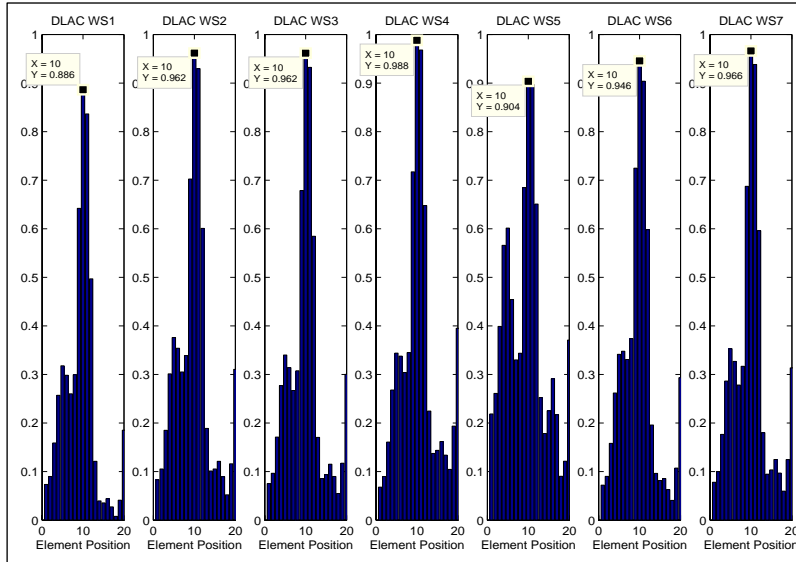


Fig 7. DLAC results for element position # 10

Mode	WS1	WS2	WS3	WS4	WS5	WS6	WS7
1	0.4767	0.4998	0.5030	0.5167	0.4806	0.4925	0.5101
2	3.8829	3.8889	3.9201	3.8785	3.8450	3.9297	3.9071
3	10.6125	10.6045	10.5549	10.6421	10.4151	10.5883	10.6263
4	22.2777	22.2284	22.2484	22.2936	21.8712	22.2304	22.2407
5	36.4255	36.3849	36.4066	36.4745	35.8035	36.3518	36.4494

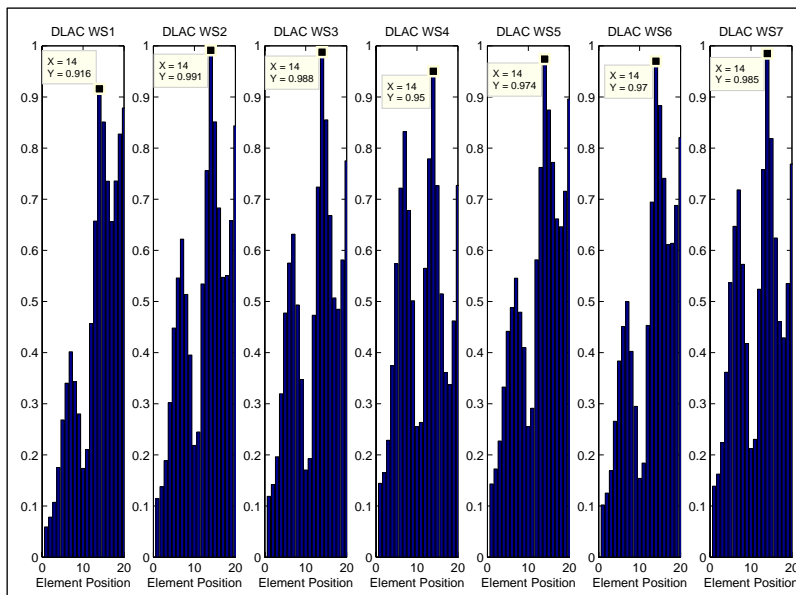


Fig 8. DLAC results for element position # 14

#### 4.2 EXPERIMENT 2: 3D Truss Structure

Preliminary results are presented for an experimental validation of the DLAC algorithm on a three-dimensional truss structure using a wireless sensor network. A 5.6 m long steel truss structure (Clayton, 2002) is tested at the Smart Structure Technology Laboratory (SSTL) at the University of Illinois at Urbana-Champaign (see Fig. 9). The specimen consists of 14 bays, each one with 0.4 m of length, sits on four rigid supports. Two supports, located at one end of the truss, are pinned-supported and able to rotate freely with all three translations restricted. The other two supports, located at the other end of the truss, are roller-supported and able to translate only in the longitudinal direction of the truss. Each of the truss members has a tube cross section with an inner diameter of 1.09 cm and outer diameter of 1.71 cm and can be either removed or replaced for damage simulation purposes without disassembling the entire structure.



Fig. 9. 3D truss test structure

A network of eleven *iMote2* wireless sensor platforms is deployed on the frontal panel of the truss at positions observed in Fig. 10. Sensor identification numbers are defined for later interpretation of the data. Sensor boards are calibrated to measure vertical acceleration data with a sampling frequency of 560 Hz and corresponding cutoff frequency of 140 Hz.

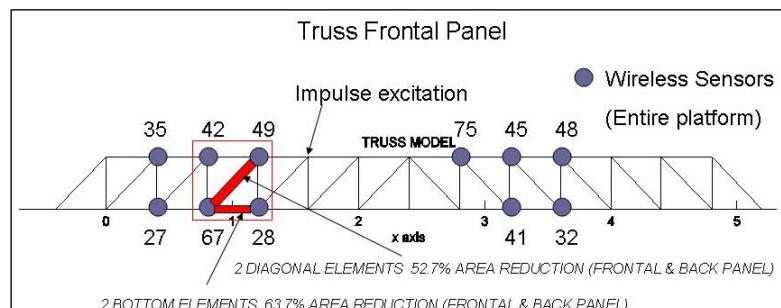


Fig 10. Truss experiment set up

Because the truss is expected to exhibit fairly complex dynamical behavior, modal identification is performed to accurately capture the dominant longitudinal bending modes in the system. The eigensystem realization algorithm (ERA) (Juang, 1985) is used to perform the modal identification analysis by processing impulse response records. A magnetic shaker that can generate a maximum force of 20 lb with a dynamic performance from 5 Hz to 9000 Hz is used to vertically excite the structure with a band-limited white noise up to 256 Hz. Output signals assessment is accomplished through the use of six wired sensors consecutively mounted through the entire frontal panel, each measuring vertical acceleration data with a sampling frequency of 512 Hz. Additionally, input signal estimation is carried out by the use of a force transducer, located between the magnetic shaker and the structure. The test is performed with the full set of eleven wireless sensors attached to the truss to ensure a consistent mass distribution before and after damage is added to the system. Signal processing analysis is then performed over input-output time records to obtain system transfer functions and corresponding impulse response functions. Finally, the ERA is applied to the impulse response functions to detect the dominant modes. Natural frequencies, reported by ERA and associated to the first five dominant bending modes, are depicted in Table 5.

Table 5. Experimental healthy natural frequencies

Mode	1	2	3	4	5
Wn	20.65	41.49	64.59	69.41	95.51

A numerical model is created to produce needed analytical damage patterns in accordance with the DLAC algorithm. A 3D Bernoulli beam element with transverse, rotational, torsion and axial degrees of freedom is selected to produce a consistent mass matrix finite element model with 160 beam elements and 336 global degrees of freedom (see Fig. 11). Boundary conditions are modeled in agreement to the actual boundary conditions of the truss mentioned in the prior section. 3 translational and 3 rotational degrees of freedom are defined for each structural node and an additional mass of 1 kg is lumped at every translational DOF to account for inertial effects induced by the steel joints. Structural damage is initially planned to be simulated by the replacement of a diagonal member with another member of reduced area. However, simulations on the analytical model using available experimental data generated in a previous research (Gao, 2005) demonstrated that the proposed damage scenario produces an insignificant modal content variation so that the damage can not be clearly detected by correlations. Therefore, a more effective damage scenario is simulated by replacing four members of the third central bay on both the frontal and back truss panels at positions depicted in Figs. 10 and 11. Diagonal members are replaced with members with a 52.7% reduced area and bottom elements are replaced with members with a 63.7 % reduced area.

The numerical model is then used to produce an analytical damage pattern of 12 damage scenarios corresponding to the 12 central bays of the truss. Each analytical damage scenario is simulated by replacing a set of 4 members in each central bay at element positions corresponding to the experimental damage with the same area section reduction. Therefore in this preliminary study, a damage hypothesis identical to the actual damage is used to produce a damage detection pattern for correlation comparisons. Finally, a sensitivity matrix containing information about the first five bending natural frequencies over 12 damage scenarios is calculated. Real damage, placed at the third central bay of the truss, is associated with the third position on the damage detection pattern. Therefore, final correlation results are expected to be closest to unity on that position due to the presence of damage.

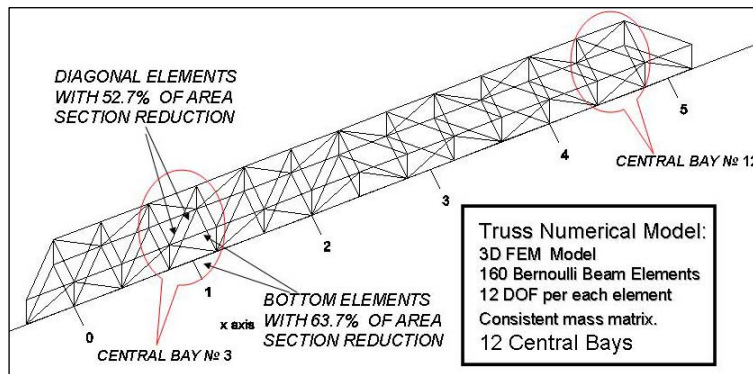


Fig 11. Truss finite element model

Analytical natural frequency results for healthy and damage cases are depicted in Table 6.

Table 6. Analytical natural frequencies

Mode	1	2	3	4	5
Healthy	19.88	38.31	66.26	67.17	92.25
Damaged	19.19	38.35	63.58	66.30	90.96

Experimental and analytical natural frequency values demonstrate good agreement. Small differences ranging from 7% to 2% can be explained due to numerical assumptions on the analytical model. Boundary conditions, homogeneous distribution for density and constitutive laws, and no numerical modelling for sensor platforms are the most important causes for those small discrepancies. Damage is then induced in the truss to validate the DLAC performance under the one scenario already described. Impact testing is selected to perform the validation by applying a hammer strike perpendicular to the longitudinal axis of the truss. After processing data, only 7 of the 11 sensors reported successful natural frequencies with DLAC results showing 85% of correlation. Results depicted in Table 7 and Fig 12, show identified natural frequencies and correlation values with a DLAC distribution along the 12 central bays. The actual damage position should be associated with truss bay # 3, since replaced elements are located on the third central bay. Although damage hypothesis equivalent to actual damage was assumed for this preliminary application, off-line analysis are conducted using raw data to test the DLAC performance under different damage assumptions. A new sensitivity matrix and corresponding frequency change vectors were developed with a prescribed analytical damage equivalent to 70% of area section reduction for all the truss members associated to the actual damage. The results show the same tendency and consistency by detecting every expected damage position.

Table 7. Identified natural frequencies

Mode	WS #32	WS #45	WS #67	WS #28	WS #35	WS #75
1	20.2718	20.2795	20.1952	20.1685	20.3122	20.2254
2	41.3708	41.4002	41.2871	41.2315	41.2998	41.2947
3	63.0427	63.1657	63.0138	63.0467	63.1021	63.0198
4	67.7883	67.8858	67.6658	67.6792	67.7284	67.6820
5	94.8858	95.0803	94.8184	94.7336	94.8865	94.8080

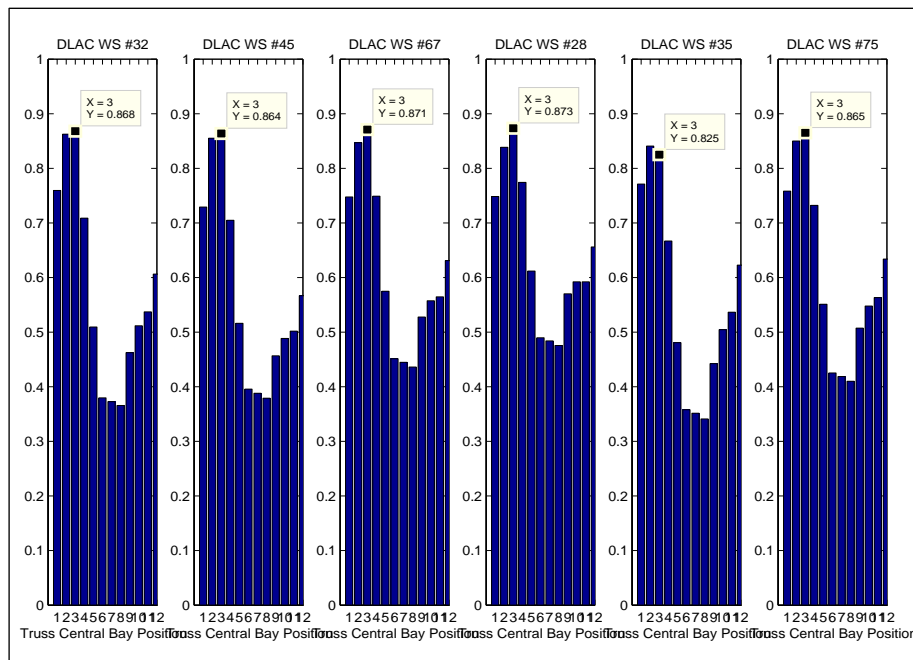


Fig 12. DLAC results for truss bay # 3

## 6.0 CONCLUSIONS

In this study a successful demonstration for an in-situ experimental validation of a correlation-based decentralized damage detection technique using a wireless sensor network has been performed. Structural damage was detected with sufficiently high correlation percentage in two experimental structures independently of the damage hypothesis used in the sensitivity matrix. On-board processing *iMote2* capacities were exploited to reduce communication load and make the application scalable within a wireless sensor network.

## 7.0 ACKNOWLEDGMENT S

Funding for this research is provided in part by the National Science Foundation; grant NSF NeTS-NOSS Grant CNS-0627126, by Washington University in St. Louis. Additionally, the authors would like to thank Prof. Bill Spencer and Shin-Ae Jang for the use of and assistance with the experimental truss.

## 8.0 REFERENCES

- Clayton, E.H. (2002), "Development of an Experimental Model for the Study of Infrastructure Preservation", *Proceedings of the National Conference on Undergraduate Research, Whitewater, Wisconsin.*
- Clayton, E.H., Koh, B.H., Xing, G., Fok, C.L., Dyke, S.J. and Lu, C. (2005), "Damage Detection and Correlation-based Localization Using Wireless Mote Sensors", *Proceedings of '05 The 13<sup>Th</sup> Mediterranean Conference on Control and Automation, Limassol, Cyprus.*
- Clayton, E.H. (2006), "Frequency Correlation-based Structural Health Monitoring with Smart Wireless Sensors", Master of Science Thesis, Washington University in St. Louis.

Contursi, T., Messina, A., Williams, E.J. (1998), "A multiple-damage location assurance criterion based on natural frequency changes", *Journal of Vibration and Control*, No.4, pp 619-633.

Crosbow Technologies iMote2 Mote IPR2400 :

<http://www.xbow.com/Products/productdetails.aspx?sid=253>

Gao, Y. (2005), "Structural Health Monitoring Strategies for Smart Sensor Networks", Doctor of Philosophy Thesis, The University of Illinois at Urbana-Champaign.

Juang, J.N. and Pappa, R.S. (1985), "An eigensystem realization algorithm for modal parameter identification and model reduction", *J. of Guidance Control and Dyn.*, 8:620-627

Koh, B.H. and Ray L.R. (2004), "Feedback controller design for sensitivity-based damage localization", *Journal of Sound and Vibration*, Vol.273, No.1-2, pp. 317-335

Messina, A., Jones, I.A. and Williams, E.J. (1996), "Damage detection and localization using natural frequencies changes", *Proceedings of Conference on Identification in Engineering Systems*, Swansea, U.K., pp 67-76.

Nagayama, T., Rice, J.A. and Spencer, B.F. Jr. (2006), "Efficacy of Intel's Imote2 wireless sensor platform for structural health monitoring applications", *Proceedings of Asia-Pacific Workshop on Structural health Monitoring*, Yokohama, Japan.

Nagayama, T. (2007), "Structural health Monitoring Using Smart Sensors", Doctor of Philosophy Thesis, The University of Illinois at Urbana-Champaign.

STMicroelectronics LIS3L02DQ data Sheet (2005):

<http://www.st.com/stonline/products/literature/od/10175/lis3l02dq.pdf>

TinyOS: <http://www.tinyos.net/>